



HAL
open science

Performances of Density Functional Tight-Binding Methods for Describing Ground and Excited State Geometries of Organic Molecules

Arnaud Fihey, Denis Jacquemin

► **To cite this version:**

Arnaud Fihey, Denis Jacquemin. Performances of Density Functional Tight-Binding Methods for Describing Ground and Excited State Geometries of Organic Molecules. *Journal of Chemical Theory and Computation*, 2019, 15 (11), pp.6267-6276. 10.1021/acs.jctc.9b00688 . hal-02364861

HAL Id: hal-02364861

<https://univ-rennes.hal.science/hal-02364861>

Submitted on 3 Feb 2020

HAL is a multi-disciplinary open access archive for the deposit and dissemination of scientific research documents, whether they are published or not. The documents may come from teaching and research institutions in France or abroad, or from public or private research centers.

L'archive ouverte pluridisciplinaire **HAL**, est destinée au dépôt et à la diffusion de documents scientifiques de niveau recherche, publiés ou non, émanant des établissements d'enseignement et de recherche français ou étrangers, des laboratoires publics ou privés.

1
2
3
4
5
6
7
8
9
10
11
12
13
14
15
16
17
18
19
20
21
22
23
24
25
26
27
28
29
30
31
32
33
34
35
36
37
38
39
40
41
42
43
44
45
46
47
48
49
50
51
52
53
54
55
56
57
58
59
60

Performances of Density Functional Tight-Binding Methods for Describing Ground and Excited State Geometries of Organic Molecules

Arnaud Fihey^{*,†} and Denis Jacquemin^{*,‡}

[†]*Institut des Sciences Chimiques de Rennes, UMR 6226 CNRS, Université de Rennes 1, 263
Av. du Général Leclerc, 35042, Cedex Rennes, France*

[‡]*Laboratoire CEISAM - UMR CNRS 6230, Université de Nantes, 2 Rue de la Houssinière,
BP 92208, 44322 Nantes Cedex 3, France*

E-mail: Arnaud.Fihey@univ-rennes1.fr; Denis.Jacquemin@univ-nantes.fr

Phone: +32 (0) 2 23 23 73 58; +32 (0) 2 51 12 55 64

Abstract

We present a benchmark of the performances of Density Functional Tight-Binding model (DFTB) and its Time-Dependent counterpart (TD-DFTB) in describing both the ground state (GS) and excited state (ES) geometries of a panel of 30 organic molecules. Thanks to high-level wavefunction reference calculations, we are able to quantitatively assess the strengths and weaknesses of four DFTB models, using either a second- or third-order Self-Consistent Charges procedures, as well as different sets of parameters. The performances of the different DFTB models are found to be largely dependent on the type of bond considered, but the global mean absolute error remains acceptable for such “cheap” quantum mechanic calculations, as it slightly exceeds the

one obtained with DFT (PBE and B3LYP) or CC2 models for the GS of the same set of compounds. When considering the ES of the molecules, the TD-DFTB errors are surprisingly not systematically larger than their GS counterparts. However, the trends, either when going from the GS to the ES, or within a homologous chemical series, are less consistently reproduced with DFTB than with the *ab initio* models. This work therefore validates the use of TD-DFTB for describing ES geometries while highlighting that care has to be applied when looking at subtle variations.

1 Introduction

Modeling photo-induced phenomena in large organic compounds over long timescales remains a key challenge in computational chemistry. Indeed, this requires the description of experimental systems encompassing photoactive molecule(s) within a complex environment, i.e., interacting with a grafting support (surface, nanoparticle), an embedding matrix (solvent, polymers), or other molecules in their vicinity. The fields of photovoltaics, sensing for medical applications, and optical information storage stand as typical examples in which the excited state (ES) events should be understood and controlled. If the vertical ES properties of isolated organic molecules (encompassing up to ca. 100 atoms) can nowadays be described with Time-Dependent Density Functional Theory (TD-DFT) for a reasonable accuracy/effort ratio,^{1,2} exploring the excited state potential energy surfaces of large compounds rapidly becomes out of reach for *ab initio* approaches. In this context, the use of the so-called “Density-Functional Tight-Binding” (DFTB) framework^{3,4} appears to be an appealing alternative. DFTB is a quantum mechanics semi-empirical scheme, that is rooted in DFT and inherits its versatility, while allowing saving ca. 99% of the computational effort by pre-computing (at the DFT/PBE level of theory) and tabulating, as parameters, the two-electrons integrals needed to solve the Kohn-Sham equations. DFTB can be viewed as an improvement of the well-known Hückel model, as matrix elements are already known, making the calculation task reduced to a matrix diagonalization and eigenvalues search problem. Among the different

1
2
3 versions of DFTB available, the most popular formalism is the Self-Consistent Charges DFTB
4 (SCC-DFTB).^{5,6} It relies on the variation of the atomic charges to iteratively search for the
5 answer of the tight-binding problem while allowing charge transfer to occur between atoms
6 as well as between orbitals of the same atom. This self-consistent modification of the DFTB
7 energy with atomic charges is determined through a second or third order Taylor expansion
8 of the DFT energy around a reference density (usually the sum of atomic densities), leading
9 respectively to the SCC-DFTB2⁵ and SCC-DFTB3^{7,8} models, simply denoted “DFTB2” and
10 “DFTB3” in the following.

11
12
13
14
15
16
17
18
19 The accuracy of DFTB methods is by construction depending on the quality of the pa-
20 rameterization used and a specific application should ideally require its own set of parameters.
21 Nevertheless, one can expect the SCC-DFTB parameters to be transferable to a certain extent.
22 Within this duality, both specific and general parameter sets have been proposed during
23 the last two decades and one can now study inorganic compounds,^{9,10} organic systems,^{11,12}
24 as well as hybrid organic-inorganic materials.^{13,14} Concerning organic molecules, the most
25 widely used set of DFTB2 parameters is by far the *mio* set,^{5,15,16} covering the interactions
26 between C, H, O, N, S, and P. Ground state (GS) properties have been extensively tested with
27 the DFTB2/*mio* approach: the obtained geometries and electronic structure properties are
28 generally in good to very good agreement with DFT results.¹¹ This *mio* set has been extended
29 to the description of halogen atoms thanks to the development of the *halorg* parameters.¹⁷
30 Another popular set of parameters is the *matsci* set that is designed not only to describe
31 inorganic solids with DFTB2 but also hybrid materials encompassing organic molecules.^{18,19}
32 In this latter set, the interactions between C, N, O, and H are available. More recently, the
33 *3ob* set has been developed to work together with the DFTB3 model and includes parameters
34 for organic atoms (C, N, O, H, P, and S),^{8,20} alkaline and alkaline earth atoms (Ca, K, Na, and
35 Mg), as well as halogens (F, Cl, Br, and I),^{21,22} improving the overall accuracy as compared
36 to the DFTB2 sets. Finally, the latest extension of DFTB is the development of formulations
37 relying on range-separated DFT functionals rather than semi-local functionals during the
38
39
40
41
42
43
44
45
46
47
48
49
50
51
52
53
54
55
56
57
58
59
60

1
2
3 parameterization process,^{23,24} in order to avoid the overdelocalization and spurious electronic
4 states typically observed with DFTB2 in large systems . This new “Long-range Corrected
5 DFTB2” (LC-DFTB2) is today available for a few atoms, namely C, H, N, and O, within
6 the *ob2* parameter set designed for organic and biological systems.²⁵
7
8
9

10
11 During the last few years, the SCC-DFTB formalism has been constantly extended, and
12 now includes many of the popular features of DFT including a Time-Dependent version,²⁶
13 empirical corrections for dispersion,^{27,28} and continuum approaches to estimate bulk solvent
14 effects.^{29,30} More specifically, the Time-Dependent DFTB (TD-DFTB)²⁶ formalism, that
15 has been available for almost two decades, allows not only bypassing the computational
16 bottlenecks of TD-DFT in the calculation of vertical excitations but also grants more efficient
17 ES geometry optimizations, thanks to the implementation of TD-DFTB analytical gradients.³¹
18 We underline that TD-DFTB calculations do not require any additional parameters besides
19 those needed for the GS, so that the above-cited sets designed for organic molecules can be
20 straightforwardly used to explore various experimental photochemistry problems. However,
21 to date, only a few works have already applied the TD-DFTB model to organic-based
22 compounds, e.g., to compute the absorption spectra of flavonol derivatives interacting with
23 boron nanotubes,³² to describe the isomerization of a pyrene molecule,³³ or to probe excited
24 state intramolecular proton transfer.³⁴ One explanation for this relatively small number of
25 TD-DFTB works is that it constitutes a relatively unexplored computational tool for the
26 community with a yet unclear applicability. Indeed, extensive studies of the TD-DFTB
27 performances remain scarce in the literature, besides the original validations to be found
28 in the theoretical works introducing the TD-DFTB extensions for DFTB2, DFTB3 and
29 LC-DFTB2.^{26,30,34-37} This is especially the case for excited state geometries, for which few
30 comparative data are available,^{31,34,36,38} although one should mention the 2004 investigation
31 of Wanko *et al.*, who investigated the potential energy surfaces of several hallmark organic
32 molecules (benzene, polyenes, protonated Schiff bases...) with TD-DFTB2.³⁸ They concluded
33 that such level of theory is reliable for the geometries when standard DFT can be trusted,
34
35
36
37
38
39
40
41
42
43
44
45
46
47
48
49
50
51
52
53
54
55
56
57
58
59
60

1
2
3 and that the two approaches have similar limitations in both accuracy and applicability.
4

5 In the present work, we provide an assessment of several DFTB variants for GS and ES
6 geometrical parameters. As in all benchmarks, the quality of the reference values is of prime
7 importance to obtain reliable conclusions. If one can easily find a plethora of experimental
8 GS geometries, this does not hold for the ES, for which the reported “measured” values
9 are often deduced from quite complex fitting procedures of the vibronic spectra, rendering
10 the final error bars non-negligible. For instance, for formaldehyde, a small and intensively
11 investigated compound, the experimentally reported estimates for the puckering angle in the
12 lowest singlet ES are 20.5° ,³⁹ 31.1° ,³⁹ and 34.0° .⁴⁰ Strikingly, the two former values have been
13 obtained in the same work,³⁹ by analyzing two different bands, 0^0 and 4^1 , respectively. In fact,
14 accurate experimental geometries are mostly available for di- and tri-atomics only. Whilst
15 these data have been used as reference,³⁶ such compounds remain far from the one used in
16 DFTB applications and, more importantly, these data are too limited to allow determining
17 statistically-relevant conclusions for different types of bonds. Therefore, at least for the
18 ES, it is safer to rely on theoretically-determined geometries. The natural choice would
19 be to select TD-DFT geometries to assess DFTB, an approach indeed applied previously
20 in the original papers introducing the various TD-DFTB models.^{30,31} However, in a recent
21 work, one of us has shown that the accuracy of the geometries obtained with TD-DFT
22 (ES) tends to be significantly smaller than with DFT (GS).⁴¹ We have therefore to select
23 reference geometries determined with highly-accurate wavefunction approaches and large
24 atomic basis sets. It was shown that both the GS and ES structural parameters obtained
25 with CCSDR(3),⁴² CC3,^{43,44} and CASPT2,^{45,46} are highly consistent when selecting active
26 spaces encompassing all valence electrons for the latter approach.⁴⁷ For instance, for the
27 puckering angle in formaldehyde the CCSDR(3), CC3, CASPT2, and CCSDT values are
28 36.6° , 36.8° , 38.2° , and 37.3° , respectively,^{41,47} that is, they span over a significantly tighter
29 range of values than their experimental counterparts (*vide supra*). We therefore select such
30 highly accurate references here. The DFTB GS and ES geometries under study result from
31
32
33
34
35
36
37
38
39
40
41
42
43
44
45
46
47
48
49
50
51
52
53
54
55
56
57
58
59
60

four different models: DFTB2 associated with the *mio* set and the *matsci* set, DFTB3 model using the *3ob* set and LC-DFTB2 with the *ob2* parameters. The results presented here are first discussed in details for a few representative cases before providing a statistical analysis.

2 Computational Details

2.1 Reference Geometries

A list of reference geometries obtained at high level of theory for 30 small and medium organic compounds (34 excited states) are gathered in the Supporting Information (SI). We consider here valence singlet ES in closed-shell compounds, a selection justified as DFTB is designed for such states in larger compounds, and not for Rydberg or open-shell states. The vast majority of our reference geometrical parameters are extracted from Refs. 41, 47, and 48. These parameters are mainly determined at the CC3 or CCSDR(3) levels of theory using large basis sets, CASPT2 reference structures being used when significant multi-reference effects are at play. Large triple- ζ basis sets, namely, *def2-TZVPP* and *aug-cc-pVTZ* have been used in all cases. In Tables S1–S7 in the SI, we report a few additional/improved reference values obtained here. The methods, algorithms, and programs used to obtain these new data are exactly the same as in our previous works.^{41,47,48} We therefore refer the interested readers to these previous investigations for further technical details.

2.2 DFTB calculations

All DFTB2/DFTB3 and TD-DFTB2/TD-DFTB3 calculations are conducted using the 18.2 version of the DFTB+ software,⁴⁹ while the LC-DFTB2 and LC-TD-DFTB2 results were obtained using a development version of GAMESS-US containing the new implementation of the range-corrected formalism recently published by Nishimoto.³⁰

For both the GS and the ES, all geometry optimizations are made using the reference wavefunction geometries as starting point and frequency calculations are performed to assess

1
2
3 if the structures correspond to global minima. Residual imaginary frequencies are specified
4 in the Tables given in the SI. Tight convergence criteria are applied to the forces in the
5 geometry optimization and charges variations within the SCC procedure, 10^{-6} and 10^{-8}
6 au, respectively. Symmetry is not explicitly taken into account during DFTB calculations.
7
8 The point group of the different compounds in their GS and ES is identified afterwards,
9 by verifying that the optimized geometry fall strictly into the point group symmetry. For
10 DFTB2 calculations, *mio* set is used for compounds containing C, H, N, O, S, F, Cl, and Br
11 atoms. Halogens parameters are taken from the *halorg* set, which is fully consistent with *mio*.
12 Therefore, in the following, the “DFTB2/*mio*” model refers to a combination of *mio* and
13 *halorg* parameters when halogens atoms are present. The *matsci* parameters are used within
14 DFTB2 for molecules containing C, H, N, and O atoms only, as sulfur and halogen atoms
15 are not described within this set. The *3ob* set applied for the DFTB3 calculations covers
16 the C, H, N, O, S, F, Cl, and Br atoms. In DFTB3, it is possible to include an additional
17 damping parameter to correct the coulombic interaction between hydrogen atoms and heavy
18 atoms.⁵¹ This correction has been demonstrated to improve the binding energies and proton
19 affinities in hydrogen bonding cases, but has trifling impact on covalent interactions. In the
20 DFTB3 results presented here, no damping is used by default except for the pathological case
21 of nitrosomethane (see below) where a damping value of 4.05 (exponent, unitless) is used in
22 agreement with the *3ob* specifications.⁵¹ Finally, the *ob2* set of parameters²⁵ was used for
23 LC-DFTB2 calculations. Only C, H, N, and O atoms are currently described in this set, and
24 molecules containing sulfur and/or halogens atoms cannot be treated at the LC-DFTB2 level
25 at this stage. The range-separation parameter, ω , needed as an input for these calculations
26 was set to $0.3/a_0$, the value optimized for the *ob2* set.²⁵
27
28
29
30
31
32
33
34
35
36
37
38
39
40
41
42
43
44
45
46
47
48
49
50

51 **2.3 *Ab initio* Calculations**

52
53 To provide a fair assessment of the quality of DFTB with respect to other methods, we have
54 also compared our reference geometrical parameters to TD-(PBE),⁵² (TD-)B3LYP⁵³⁻⁵⁶ and
55
56
57
58
59
60

(LR-)CC2^{43,57,58} results for all compounds. Please note that PBE is the functional used to parametrize DFTB2 and DFTB3 and is thus included here as a reference for a more direct evaluation of potential pitfalls of the tight-binding approach originating from the underlying DFTs. Full results are available in the SI. Some PBE, B3LYP and CC2 values could be taken from literature (see the SI), but new calculations have to be made in the present work. All our DFT computations are performed with the Gaussian16 code with the *aug-cc-pVTZ* basis set.⁵⁹ We first optimize both the GS and ES geometries (starting with the coordinates obtained at the reference level of theory) until the residual mean square force is below the 1×10^{-5} au threshold, before analytically determining the vibrational frequencies to ascertain the nature of the minima (when an instability is noted, this is indicated in the SI). These calculations use a (99,590) pruned integration grid (*ultrafine*) and rely on an improved energy convergence threshold (ca. 10^{-9} au). The CC2 calculations are done with Turbomole,⁶⁰ selecting the *aug-cc-pVTZ* basis set and taking advantage of the resolution-of-identity (RI) approach. During the CC2 calculations, the SCF, second-order, and geometry optimization thresholds are respectively tightened to 10^{-9} au, 10^{-7} au and 10^{-5} au, and all electrons are correlated. Numerical vibrational frequency calculations are also performed at the CC2 level of theory.

3 Results and Discussion

3.1 Selected examples

Before discussing in the next Section the statistical results obtained with DFTB2/*mio*, DFTB2/*matsci*, DFTB3/*3ob*, and LC-DFTB2/*ob2*, and comparing them to DFT and CC2 data, let us briefly present a few representative examples. First in the vast majority of cases, it is possible to obtain both the GS and ES structures with all DFTB approaches without specific difficulties. There are a few exceptions to this general statement. For both formylchloride and phosgene, the optimizations of the lowest ES lead to an unphysical extension of the

1
2
3 C-Cl bond(s) with DFTB, which is incorrect as these ES have been characterized in gas
4 phase experimentally.⁶¹⁻⁶³ It is noteworthy that the same dissociative behavior is obtained
5 with B3LYP for formylchloride (but no phosgene), whereas coupled cluster approaches (and
6 TD-DFT with many other functionals) are more successful.^{41,47} In some cases, the symmetry
7 of the ES differs in the reference approach and in DFTB. An interesting case is nitrosomethane,
8 a molecule for which experimental evidences indicate an eclipsed GS conformation but a
9 staggered minimum after transitions to the lowest ES.^{64,65} Such rotation of the methyl group
10 upon excitation is accurately reproduced by PBE, B3LYP, CC2, and CC3 (Table S32 in the
11 SI). The same holds for (LC-)DFTB2 (with all parameter sets), but not with DFTB3/*3ob*
12 that yields an imaginary frequency for the eclipsed GS, an error that can be corrected by using
13 a H-X (X: heavy atom) damped interaction approach (see computational details). In this case
14 the presence of the oxygen atom relatively close to one of the hydrogen atoms of the methyl
15 may hint at potential weak interactions missing or incompletely described in DFTB3 without
16 additional damping parameter. However, the fact that DFTB2 is able to retrieve the correct
17 conformations renders quite unclear the need of higher level electrostatic perturbation models,
18 and pinpoints instead to some error compensation phenomenon. For thioformylchloride, the
19 reference experimental work⁶⁶ as well as high-level CC⁴⁷ and multi-reference^{47,67} calculations
20 point out at a slight puckering of the ES, which could be qualitatively reproduced with
21 DFTB3/*3ob* but not with DFTB2/*mio* that predicts a planar ES (Table S40 in the SI). At
22 the TD-DFT level, the same "flattening" problem is obtained with functionals including a
23 large ratio of *exact* exchange, e.g., M06-2X and ω B97X, but not with B3LYP.⁴¹
24
25
26
27
28
29
30
31
32
33
34
35
36
37
38
39
40
41
42
43
44

45 In Table 1 we list selected geometrical parameters for the homologous formaldehyde,
46 acetaldehyde, and acetone series (see SI for complete data). All tested DFTB models correctly
47 foresee a strong elongation of the carbonyl bond lengths accompanied by a significant puckering
48 after the $n \rightarrow \pi^*$ transition. In addition, in the GS, the CO bond length is accurately
49 estimated by all methods, and one notes that LC-DFTB2 provides longer carbonyl lengths
50 than the other DFTB methods, especially for formaldehyde. All approaches also predict
51
52
53
54
55
56
57
58
59
60

1
2
3 a slight lengthening of this bond when going from formaldehyde to acetone but this effect
4 seems exaggerated with DFTB (+0.005 Å according to CCSDR(3) *versus* +0.025 Å with
5 DFTB2/*mio*). For formaldehyde, the elongation of the bond in the ES is estimated to be
6 +0.113 Å with CCSDR(3), a value inline with the most recent experiments,^{40,68} as well as
7 with previously reported MR-AQCC⁶⁹ and CR-EOM-CCSD(T)⁶⁷ studies. Consistently with
8 our previous work,⁴¹ both PBE and B3LYP slightly underestimates this change, whereas
9 DFTB overestimates it, quite strongly in the case of the DFTB2/*matsci* parameters (+0.167
10 Å). The evolution of this ES lengthening with the addition of methyl groups seems also
11 exaggerated with DFTB as compared to CCSDR(3). For the puckering angle, a parameter
12 that is very sensitive to the level of theory and challenging for experiment (see Introduction),
13 our theoretical best estimates are ca. 37–38° for formaldehyde and acetaldehyde but 42° for
14 acetone. Such trend is correctly restored by B3LYP though this functional systematically
15 provides too small angles (33–34° and 37°). PBE does not provide such an accurate trend, but
16 delivers errors smaller than 10° in all cases. All tested DFTB parameterizations provide an
17 incorrect trend with a strong decrease of this puckering upon addition of methyl groups (ca.
18 -10° per methyl group). As a consequence, DFTB reasonably estimates the puckering angle in
19 acetaldehyde but returns rather large errors for formaldehyde (overestimation) and acetone
20 (underestimation), with absolute errors larger than with PBE. For acetone, the LC-DFTB2
21 puckering angle is too small by 25°. This is a first illustration that while DFTB provides,
22 on average, rather accurate geometrical parameters, the evolution in a homologous chemical
23 series, i.e., the consistency, is less satisfying than with standard hybrid DFT approaches.
24
25
26
27
28
29
30
31
32
33
34
35
36
37
38
39
40
41
42
43
44

45 In Table 2, we present the results obtained for two compounds in which the lowest
46 transition presents a $\pi \rightarrow \pi^*$ character. In benzene, the CC bond length as well as its
47 elongation upon excitation are consistently given by all approaches, although LC-DFTB2/*ob2*
48 yields a slightly too long GS bond length, but an accurate extension in the ES. For the CH
49 bonds, DFTB accurately predicts negligible changes from the GS to the ES but yields too
50 long GS distances, especially with the two DFTB2 parameterizations, e.g., the GS CH bond
51
52
53
54
55
56
57
58
59
60

Table 1: Selected geometrical parameters for formaldehyde, acetaldehyde, and acetone determined with several methods. We provide the C=O bond length in the GS, and its elongation in the lowest singlet ES in parenthesis (in Å), as well as the ES puckering angle (η in degrees).

Method	C=O			η		
	H ₂ C=O	MeHC=O	Me ₂ C=O	H ₂ C=O	MeHC=O	Me ₂ C=O
DFTB2/ <i>mio</i>	1.183 (+0.137)	1.196 (+0.151)	1.208 (+0.167)	53.3	42.9	31.2
DFTB2/ <i>matsci</i>	1.192 (+0.167)	1.204 (+0.176)	1.216 (+0.188)	55.2	43.6	26.0
DFTB3/ <i>3ob</i>	1.183 (+0.121)	1.204 (+0.129)	1.215 (+0.142)	55.3	44.7	32.2
LC-DFTB2/ <i>ob2</i>	1.206 (+0.115)	1.211 (+0.141)	1.219 (+0.135)	40.0	33.8	17.6
PBE	1.210 (+0.096)	1.215 (+0.103)	1.221 (+0.106)	38.6	34.0	34.5
B3LYP	1.200 (+0.092)	1.204 (+0.096)	1.210 (+0.096)	33.8	33.5	36.7
CCSDR(3) ^a	1.207 (+0.113)	1.209 (+0.118)	1.212 (+0.120)	36.6	37.9	42.3
Exp ^b	1.207 (+0.116)	1.21 (+0.11)		34	26	

^aCCSDR(3)/*aug-cc-pVTZ* values from Refs. 47, 41, and the present work for formaldehyde, acetaldehyde and acetone, respectively. ^bMost recent (collection of) experimental data we are aware of: Ref. 40 for formaldehyde and Ref. 70 for acetaldehyde.

length is 1.098 Å with DFTB2/*mio* but 1.081 Å with CCSDR(3)/*def2-TZVPP*. For the GS geometry of cyanogen (N≡C–C≡N), DFTB, PBE and B3LYP all predict C≡N bonds with errors of ca. 0.010 Å, an acceptable deviation, LC-DFTB2 being significantly more efficient. In contrast, the central CC bond is too long by ca. 0.015–0.025 Å with DFTB whereas both PBE and B3LYP are close to the spot. As a consequence, the bond length alternation (BLA), an important parameter for evaluating the electronic communication in π -delocalized systems reaches 0.249 Å with DFTB3/*3ob* but 0.219 Å with CC3. As for benzene, the evolution of both bond lengths upon electronic transition are quite accurately reproduced with DFTB but for a slight overestimation of the elongation of the CN triple bonds. Due to a small error compensation, the DFTB BLA are accurate for the ES, with a value of 0.071 Å with DFTB3/*3ob* close to the CC3 reference value of 0.062 Å. This shows that there is not always a degradation of DFTB’s accuracy when going the GS to the ES. One also notices for cyanogen, that the DFTB geometrical parameters are not necessarily closer to the ones obtained with PBE (the functional used to parametrize DFTB2 and DFTB3), than to the B3LYP values. In short, DFTB globally shows a satisfying performance for both benzene and cyanogen.

Table 2: Selected geometrical parameters for benzene and cyanogen determined with several methods. We provide the bond lengths in the GS, and their elongation in the selected ES (see the SI) in parenthesis (in Å). TBE is the theoretical best estimate used as reference values.

Method	Benzene		Cyanogen	
	CC	CH	CN	CC
DFTB2/ <i>mio</i>	1.396 (+0.032)	1.098 (0.000)	1.149 (+0.092)	1.406 (-0.081)
DFTB2/ <i>matsci</i>	1.393 (+0.034)	1.102 (-0.001)	1.155 (+0.098)	1.404 (-0.081)
DFTB3/ <i>3ob</i>	1.396 (+0.035)	1.088 (0.000)	1.154 (+0.098)	1.403 (-0.086)
LC-DFTB2/ <i>ob2</i>	1.402 (+0.031)	1.089 (0.000)	1.159 (+0.085)	1.395 (-0.084)
PBE	1.388 (+0.031)	1.084 (0.005)	1.167 (+0.075)	1.374 (-0.066)
B3LYP	1.391 (+0.030)	1.082 (-0.002)	1.152 (+0.078)	1.376 (-0.079)
TBE ^a	1.396 (+0.026)	1.081 (-0.002)	1.161 (+0.076)	1.380 (-0.081)

^aCCSDR(3)/*def2*-TZVPP values of this work for benzene, CC3/*aug-cc-pVTZ* data from Ref. 47 for cyanogen.

3.2 Statistical study

The results of a statistical investigation carried out for all approaches using the CC3 or CCSDR(3) geometries as reference are displayed in Table 3 that reports the mean signed (MSE) and mean absolute (MAE) errors. Note that for two ES (B_u state of acetylene and A'' of diazomethane) the CASPT2 geometry is taken as benchmark as significant multi-reference characters appear for these ES.⁴⁷ A histogram representation of the cumulative errors per bond type is available in Figure 1.

Let us start our analysis by looking at the PBE, B3LYP and CC2 statistics, for which the present results are globally inline with previous benchmarks focused on TD-DFT or post-HF methods.^{41,47,71–75} Indeed, it can be seen that: i) a higher accuracy is almost systematically obtained for the GS parameters than for the ES ones; ii) the polar CO, CN, and CX bonds are the one generating the largest errors with these three methods; iii) errors are also notably larger for CH bonds with PBE; iv) the ES carbonyl bond lengths tend to be significantly too short with B3LYP and PBE but significantly too long with CC2, which is consistent with other investigations;^{47,73,76,77} v) the MAE obtained with the three methods are alike (see Figure 1), so that using CC2 as reference to assess the accuracy of B3LYP (or other similar functionals) is probably a relatively risky approach. The standard deviations of the errors

Table 3: Mean signed and absolute errors determined for GS (top) and ES (bottom) geometrical parameters. Errors for all distances are in Å, whereas deviations are given in degrees for valence (val) and dihedral (dih) angles. CX are carbon-halogen bonds.

Method	Ground state													Excited state													
	Mean Signed Error						Mean Absolute Error						Mean Signed Error						Mean Absolute Error								
	All	CC	CO	CN	CH	CS	CX	Val	Dih	All	CC	CO	CN	CH	CS	CX	Val	Dih	All	CC	CO	CN	CH	CS	CX	Val	Dih
DFTB2/ <i>mio</i>	0.013	0.007	-0.007	-0.002	0.024	-0.008	0.064	-0.3	-	0.018	0.009	0.011	0.008	0.024	0.008	0.064	1.1	-	0.022	0.017	0.020	0.011	0.023	0.040	0.059	3.5	8.9
DFTB2/ <i>matsci</i>	0.011	0.008	0.001	-0.019	0.028	-	-	-0.1	-	0.018	0.010	0.011	0.023	0.028	-	-	1.7	-	0.024	0.017	0.028	0.029	0.028	-	-	4.1	13.4
DFTB3/ <i>3ob</i>	0.010	0.007	0.001	0.034	0.013	0.009	0.002	-0.2	-	0.014	0.009	0.009	0.040	0.013	0.014	0.014	1.9	-	0.015	0.018	0.014	0.015	0.013	0.016	0.009	3.5	7.9
LC-DFTB2/ <i>ob2</i>	0.006	0.007	0.005	-0.005	0.010	-	-	0.1	-	0.009	0.009	0.007	0.008	0.010	-	-	1.2	-	0.015	0.017	0.016	0.015	0.009	-	-	2.4	10.3
PBE	0.007	0.001	0.006	0.005	0.012	0.001	0.018	0.3	-	0.008	0.005	0.006	0.005	0.012	0.001	0.018	0.4	-	0.011	0.007	0.018	0.010	0.012	0.011	0.026	1.3	3.3
B3LYP	-0.001	-0.004	-0.005	-0.004	0.003	-0.007	0.013	0.1	-	0.005	0.005	0.005	0.005	0.003	0.007	0.013	0.3	-	0.008	0.007	0.026	0.007	0.002	0.023	0.014	1.4	3.0
CC2	0.000	-0.004	0.009	0.010	-0.002	0.000	-0.003	0.0	-	0.006	0.007	0.009	0.012	0.002	0.002	0.008	0.3	-	0.011	0.012	0.032	0.015	0.003	0.008	0.014	1.6	3.9

(STD) obtained with PBE, B3LYP and CC2 by considering all bond lengths are respectively 0.007, 0.007 and 0.009 Å in the GS, and 0.015, 0.013 and 0.019 Å in the ES. These small STD indicate rather consistent estimates, especially in the GS.

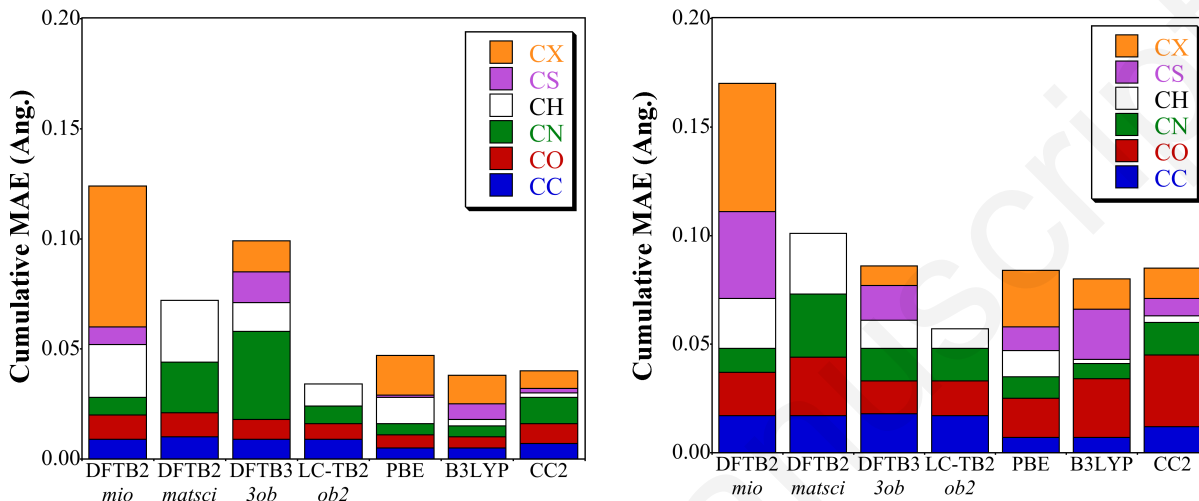


Figure 1: Cumulative mean absolute errors for the GS (left) and ES (right) for six kinds of bond lengths. All values are in Å. Note that no CS and CX errors can be determined with the DFTB2/*matsci* LC-DFTB2/*ob2* approaches is due to the lack of parameters for sulfur and halogens in these parameterizations. The total numbers of reference GS/ES parameters are 31/37 for CC, 11/11 for CO, 9/10 for CN, 25/32 for CH, 5/5 for CS, and 8/8 for CX bonds, respectively.

Let us now look at the DFTB statistical results. First, we note that using the *matsci* parameters instead of their *mio* counterparts in DFTB2 yields either equal or larger errors, which could be expected as the *mio* parameters are specifically designed to describe molecules and not materials like the former. As in addition *matsci* parameters are not available for sulfur and halogen atoms, we focus our discussion on the DFTB2/*mio*, DFTB3/*3ob* and LC-DFTB2/*ob2* results in the following.

For the GS parameters, Table 3 shows that the deviations are generally larger with DFTB than with both B3LYP and CC2. However, the average errors obtained with the DFTB schemes are rather satisfying. For all tested DFTB approaches, the MAE are indeed ca. 0.01 Å for CC, CO, and CS bonds and 1-2° for valence angles. In contrast, the CH bonds

1
2
3 seem problematic for these methods: the computed distances are significantly larger than
4 the reference values, a problem also encountered with the PBE functional. Clearly the LC-
5 DFTB2 and DFTB3 approaches provide a significant improvement as compared to DFTB2
6 (MSE of +0.024 Å with DFTB2/*mio*, +0.013 Å with DFTB3/*3ob*, and +0.010 Å with
7 LC-DFTB2/*ob2*). Whether or not these larger errors for the CH bonds with DFTB than with
8 B3LYP are a significant difficulty or not does, of course, depend on the targeted applications.
9 For the CN bonds, both DFTB2/*mio* and LC-DFTB2/*ob2* provide quite excellent results,
10 actually outperforming CC2 on the MAE, whereas DFTB3/*3ob* does not provide an accurate
11 description with rather large overestimations of the bond lengths. For carbon-halogen (CX)
12 distances, the reverse trend is found, with rather limited deviations with DFTB3/*3ob* and very
13 large errors when using the CX interactions from the *halorg* set to complete the DFTB2/*mio*
14 model (MSE of +0.064 Å). By considering all bond types, we obtain STD of 0.023, 0.031 and
15 0.009 Å with DFTB2/*mio*, DFTB3/*3ob*, and LC-DFTB2/*ob2*, respectively, values that are
16 3–4 times larger than with B3LYP (0.007 Å) for the two non-LC approaches, indicating a
17 larger spread of the deviations with these schemes. This is graphically illustrated in the left
18 panel of Figure 2 for CO bonds: while B3LYP (CC2) systematically delivers too contracted
19 (extended) carbonyl bonds, the sign of the error might change from one compound to the
20 other with the two DFTB schemes. Note that LC-DFTB2 is more coherent than the other
21 DFTB approaches but also yields different error signs for CO bonds depending on the
22 selected system, e.g., +0.014 Å for maleimide, but -0.002 Å for formaldehyde. As a conclusion,
23 using DFTB for determining the GS geometrical parameters of organic compounds is a valid
24 approach, and one can likely advise the use of the LC-DFTB2/*ob2* approach, which clearly
25 emerge as competitive for CNOH compounds, or DFTB3/*3ob* if halogens are present in
26 the compound. In addition, given its negligible computational cost compared to B3LYP or
27 CC2, DFTB turns out to be “competitive”. Indeed, if the spread of the errors is larger with
28 DFTB than with *ab initio* methods, the DFTB average deviations for the three “molecular”
29 parameterizations remain of the same order of magnitudes as with these *ab initio* approaches
30
31
32
33
34
35
36
37
38
39
40
41
42
43
44
45
46
47
48
49
50
51
52
53
54
55
56
57
58
59
60

for many bond types but for the CH and CX (with DFTB2/*mio*) or CN (with DFTB3/*3ob*) linkages that are less accurately reproduced.

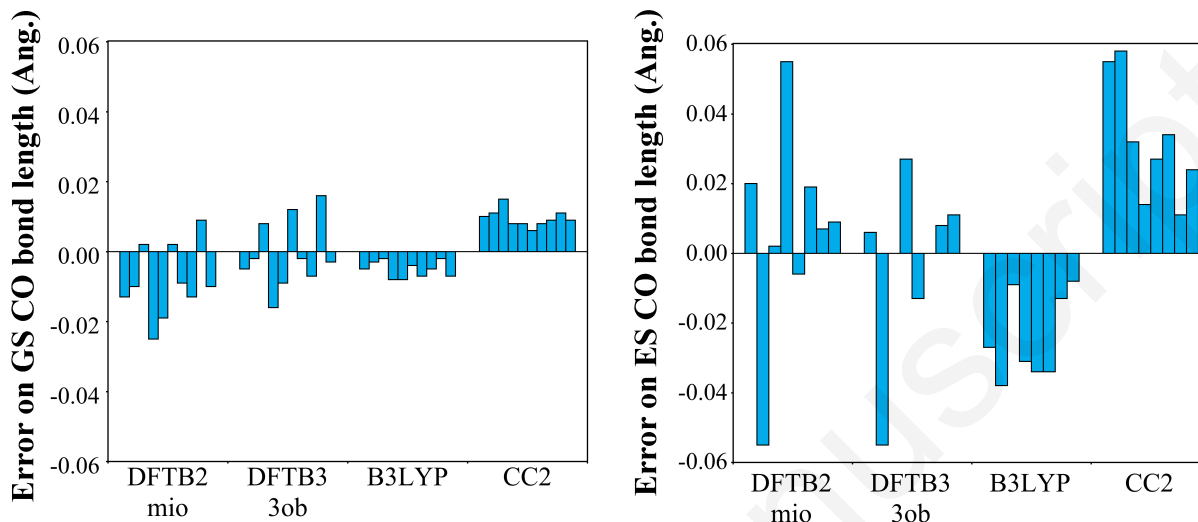


Figure 2: Representation of the errors obtained for the 10 (GS, left) and 8 (ES, right) CO bonds lengths for which all four methods lead to an optimal geometry. Each histogram represents the error made for a specific molecule, ordered in alphabetical order.

As for B3LYP and CC2, the deviations computed for the (LC-)DFTB2 geometrical parameters with respect to reference values are larger in the ES than in GS. Surprisingly, as can be seen in Figure 1, the picture is less clear for DFTB3 with improvement or degradation of the accuracy in the ES as compared to the GS depending on the considered bond type. With all DFTB approaches, the valence angles show typical errors of $2.4\text{--}4.1^\circ$, whereas the dihedral angles (related to ES puckering here) deviate by $8\text{--}10^\circ$ on average but with a quite large spread for these two parameters. For both families of angles, the DFTB results are significantly less satisfying than the DFT and CC2 ones that show twice smaller MAE than DFTB. Additionally we notice a totally systematic tendency of underestimating the puckering angles with CC2, i.e., a “consistent” error, whereas as illustrated above for the formaldehyde series, a more inconsistent behavior is found with DFTB. DFTB2/*matsci* delivers deviations of ca. $0.02\text{--}0.03 \text{ \AA}$ for all bond types for which parameters are available. With DFTB2/*mio*, the errors on CC, CO, CN, and CH bonds are ca. $0.01\text{--}0.02 \text{ \AA}$ in the ES, values that can

probably be viewed as rather satisfying, but quite large errors are found for both the CS (too short, MSE of -0.040 \AA) and CX (too long, MSE of $+0.059 \text{ \AA}$) bonds. The large errors obtained for CS bonds might be due to the parametrization for the sulfur atoms, as discussed elsewhere.⁵⁰ Consequently, the STD determined for DFTB2/*mio* ES bond lengths reaches 0.024 \AA , significantly above its B3LYP counterpart (0.013 \AA). With both DFTB3/*3ob* and LC-DFTB2/*ob2*, the obtained errors in the ES are smaller than the 0.02 \AA threshold for all bond types; the two methods even clearly outperforming CC2 for both CO bond lengths in terms of average accuracy. Although this is an additional indication that benchmarking DFTB accuracy on carbonyl bond lengths using B3LYP or CC2 is not a satisfying procedure, it should be stressed again that the errors made with DFTB are less systematic than with *ab initio* methods, as illustrated in the right panel of Figure 2 for CO bonds. In short, for ES optimization, one can most probably select DFTB3/*3ob* or LC-DFTB2/*ob2* as the average errors tend to be smaller than with the two other DFTB parametrizations.

4 Conclusions and Outlook

To the best of our knowledge, this work stands as the first in-depth comparison between the GS and ES structural parameters of organic molecules obtained with DFTB and with state-of-the-art wavefunction methods. Such benchmark strategy allows an improved assessment of the DFTB *pros* and *cons*, as one is freed from the limitations inherent to the use of reference data coming from experiment (availability, measurement procedures) or TD-DFT (accuracy, choice of a specific functional). Using a batch of 30 molecules exhibiting low-lying $n \rightarrow \pi^*$ and $\pi \rightarrow \pi^*$ electronic transitions, various heteroatoms (O, N, and S) and halogens (F, Cl, and Br), as well as diverse amplitudes of geometry changes between the GS and ES, the accuracy of four different SCC-DFTB models (DFTB2/*mio*, DFTB/*matsci*, DFTB3/*3ob* and LC-DFTB2/*ob2*) is assessed and compared to the ones of DFT and CC2.

If the average errors (MAE) are found to be larger for DFTB model than for B3LYP

1
2
3 and CC2 for the ground state, the picture is less clear for the excited state for which both
4 DFTB3 and LC-DFTB2 sometimes outperforms *ab initio* methods. As for B3LYP and CC2,
5 the DFTB ability to accurately describe the structures of organic molecules appears to be
6 dependent on the bond type. For the GS, while both CC and CO distances are satisfyingly
7 reproduced, the DFTB geometries show constantly overestimated CH distances, especially
8 in the DFTB2 framework. In contrast, DFTB2 provides relatively accurate CN distances
9 when DFTB3 returns too long CN bonds. When halogen atoms are present, the DFTB2
10 distances are largely overestimated and the use of DFTB3 appears necessary. For the GS
11 geometry of compounds with only C, N, O and H atoms, one can probably suggest the
12 use of the LC-DFTB2 approach which provides the smallest average errors and standard
13 deviations amongst the four tested DFTB models. Interestingly, the accuracy of DFTB does
14 not systematically decrease when going from the GS to the ES description. This could be an
15 advantage as compared to most *ab initio* methods. However, these errors appear to be less
16 systematic with DFTB than with B3LYP and CC2, showing larger spread, and consequently
17 making trends in a homologous series of chemical systems sometimes inaccurate. In addition,
18 this work also clearly confirms that assessing the accuracy of “low-order” computational
19 schemes without very accurate reference data might be risky, which is in line with a recent
20 work by one of us.⁷⁸

21
22
23
24
25
26
27
28
29
30
31
32
33
34
35
36
37
38
39 As an outlook, we provide in the last Section of the SI a comparison between DFTB3/*3ob*,
40 LC-DFTB2/*ob2*, and CC2 ground and excited state structures for five real-life dyes presenting
41 either charge-transfer or highly-delocalized ES. Although CC2 is not accurate enough to
42 provide a quantitative assessment (see above), it is obvious from the data of Table S42 that
43 the two tested DFTB approaches generally reproduce well the evolution of the bond distances
44 induced by electronic excitation.
45
46
47
48
49
50
51
52
53
54
55
56
57
58
59
60

Acknowledgement

The authors are indebted to Prof. Y. Nishimoto for providing the GAMESS code allowing to performed the LC-TD-DFTB2 calculations presented here. D.J. acknowledges the *Région des Pays de la Loire* for financial support. This research has been performed with resources from i) GENCI-CINES/IDRIS; ii) CCIPL (*Centre de Calcul Intensif des Pays de Loire*); and iii) Troy cluster installed in Nantes.

Supporting Information Available

Reference geometries. All considered geometrical parameters.

References

- (1) Adamo, C.; Jacquemin, D. The calculations of Excited-State Properties with Time-Dependent Density Functional Theory. *Chem. Soc. Rev.* **2013**, *42*, 845–856.
- (2) Laurent, A. D.; Adamo, C.; Jacquemin, D. Dye Chemistry with Time-Dependent Density Functional Theory. *Phys. Chem. Chem. Phys.* **2014**, *16*, 14334–14356.
- (3) Porezag, D.; Frauenheim, T.; Köhler, T.; Seifert, G.; Kaschner, R. Construction of Tight-Binding-Like Potentials on the Basis of Density-Functional Theory: Application to Carbon. *Phys. Rev. B* **1995**, *51*, 12947–12957.
- (4) Seifert, G.; Porezag, D.; Frauenheim, T. Calculations of Molecules, Clusters, and Solids with a Simplified LCAO-DFT-LDA Scheme. *Int. J. Quantum Chem.* **1996**, *58*, 185–192.
- (5) Elstner, M.; Porezag, D.; Jungnickel, D.; Elsner, J.; Haugk, M.; Frauenheim, S., Th.and Suhai; Seifert, G. Self-consistent-charge density-functional tight-binding method for simulations of complex materials properties. *Phys. Rev. B* **1998**, *58*, 7260–7268.

- 1
2
3
4 (6) Seifert, G.; Joswig, J.-O. Density-Functional Tight Binding – An Approximate Density-
5 Functional Theory Method. *Wiley Interdiscip. Rev.: Comput. Mol. Sci.* **2012**, *2*, 456–465.
6
7
8 (7) Gaus, M.; Cui, Q.; Elstner, M. DFTB3: Extension of the Self-Consistent-Charge Density-
9 Functional Tight-Binding Method (SCC-DFTB). *J. Chem. Theory Comput.* **2011**, *7*,
10 931–948.
11
12
13
14 (8) Gaus, M.; Goez, A.; Elstner, M. Parametrization and Benchmark of DFTB3 for Organic
15 Molecules. *J. Chem. Theory Comput.* **2013**, *9*, 338–354.
16
17
18
19 (9) Sieck, A.; Frauenheim, T.; Jackson, K. A. Shape Transition of Medium-Sized Neutral
20 Silicon Clusters. *Phys. Status Solidi B* **2003**, *240*, 537–548.
21
22
23
24 (10) Lourenço, M. P.; de Oliveira, C.; Oliveira, A. F.; Guimarães, L.; Duarte, H. A. Structural,
25 Electronic, and Mechanical Properties of Single-Walled Chrysotile Nanotube Models. *J.*
26 *Phys. Chem. C* **2012**, *116*, 9405–9411.
27
28
29
30
31 (11) Krüger, T.; Elstner, M.; Schiffels, P.; Frauenheim, T. Validation of the Density-Functional
32 Based Tight-Binding Approximation Method for the Calculation of Reaction Energies
33 and Other Data. *J. Chem. Phys.* **2005**, *122*, 114110.
34
35
36
37
38 (12) Gaus, M.; Cui, Q.; Elstner, M. Density Functional Tight Binding: Application to
39 Organic and Biological Molecules. *Wiley Interdiscip. Rev.: Comput. Mol. Sci.* **2014**, *4*,
40 49–61.
41
42
43
44 (13) Dolgonos, G.; Aradi, B.; Moreira, N. H.; Frauenheim, T. An Improved Self-Consistent-
45 Charge Density-Functional Tight-Binding (SCC-DFTB) Set of Parameters for Simulation
46 of Bulk and Molecular Systems Involving Titanium. *J. Chem. Theory Comput.* **2010**, *6*,
47 266–278.
48
49
50
51
52
53 (14) Fihey, A.; Hettich, C.; Touzeau, J.; Maurel, F.; Perrier, A.; Köhler, C.; Aradi, B.; Frauen-

- heim, T. SCC-DFTB Parameters for Simulating Hybrid Gold-Thiolates Compounds. *J. Comput. Chem.* **2015**, *36*, 2075–2087.
- (15) Niehaus, T.; Elstner, M.; Frauenheim, T.; Suhai, S. Application of an Approximate Density-Functional Method to Sulfur Containing Compounds. *J. Mol. Struct.: THEOCHEM* **2001**, *541*, 185–194.
- (16) Yang, Y.; Yu, H.; York, D.; Elstner, M.; Cui, Q. Description of Phosphate Hydrolysis Reactions with the Self-Consistent-Charge Density-Functional-Tight-Binding (SCC-DFTB) Theory. 1. Parameterization. *J. Chem. Theory Comput.* **2008**, *4*, 2067–2084.
- (17) Kubar, T.; Bodrog, Z.; Gaus, M.; Köhler, C.; Aradi, B.; Frauenheim, T.; Elstner, M. Parametrization of the SCC-DFTB Method for Halogens. *J. Chem. Theory Comput.* **2013**, *9*, 2939–2949.
- (18) Lukose, B.; Kuc, A.; Frenzel, J.; Heine, T. On the Reticular Construction Concept of Covalent Organic Frameworks. *Beilstein J. Nanotechnol.* **2010**, *1*, 60–70.
- (19) Gemming, S.; Enyashin, A. N.; Frenzel, J.; Seifert, G. Adsorption of Nucleotides on the Rutile (110) Surface. *Int. J. Mater. Res.* **2010**, *101*, 758–764.
- (20) Gaus, M.; Lu, X.; Elstner, M.; Cui, Q. Parameterization of DFTB3/3ob for Sulfur and Phosphorus for Chemical and Biological Applications. *J. Chem. Theory Comput.* **2014**, *10*, 1518–1537.
- (21) Kubillus, M.; Kubař, T.; Gaus, M.; Řezáč, J.; Elstner, M. Parameterization of the DFTB3 Method for Br, Ca, Cl, F, I, K, and Na in Organic and Biological Systems. *J. Chem. Theory Comput.* **2015**, *11*, 332–342.
- (22) Lu, X.; Gaus, M.; Elstner, M.; Cui, Q. Parametrization of DFTB3/3ob for Magnesium and Zinc for Chemical and Biological Applications. *J. Phys. Chem. B* **2015**, *119*, 1062–1082.

- 1
2
3
4 (23) Humeniuk, A.; Mitrić, R. Long-Range Correction for Tight-Binding TD-DFT. *J. Chem.*
5 *Phys.* **2015**, *143*, 134120.
6
7
8 (24) Lutsker, V.; Aradi, B.; Niehaus, T. A. Implementation and Benchmark of a Long-
9 Range Corrected Functional in the Density Functional Based Tight-Binding Method. *J.*
10 *Chemical Phys.* **2015**, *143*, 184107.
11
12
13
14 (25) Vuong, V. Q.; Akkarapattiakal Kuriappan, J.; Kubillus, M.; Kranz, J. J.; Mast, T.;
15 Niehaus, T. A.; Irle, S.; Elstner, M. Parametrization and Benchmark of Long-Range
16 Corrected DFTB2 for Organic Molecules. *J. Chem. Theory Comput.* **2018**, *14*, 115–125.
17
18
19 (26) Niehaus, T. A.; Suhai, S.; Della Sala, F.; Lugli, P.; Elstner, M.; Seifert, G.; Frauenheim, T.
20 Tight-Binding Approach to Time-Dependent Density-Functional Response Theory. *Phys.*
21 *Rev. B* **2001**, *63*, 085108.
22
23
24 (27) Elstner, M.; Hobza, P.; Frauenheim, T.; Suhai, S.; Kaxiras, E. Hydrogen Bonding and
25 Stacking Interactions of Nucleic Acid Base Pairs: A Density-Functional-Theory Based
26 Treatment. *J. Chem. Phys.* **2001**, *114*, 5149–5155.
27
28
29 (28) Petraglia, R.; Steinmann, S. N.; Corminboeuf, C. A Fast Charge-Dependent Atom-
30 Pairwise Dispersion Correction for DFTB3. *Int. J. Quantum Chem.* **2015**, *115*, 1265–
31 1272.
32
33
34 (29) Barone, V.; Carnimeo, I.; Scalmani, G. Computational Spectroscopy of Large Systems in
35 Solution: The DFTB/PCM and TD-DFTB/PCM Approach. *J. Chem. Theory Comput.*
36 **2013**, *9*, 2052–2071.
37
38
39 (30) Nishimoto, Y. Time-Dependent Long-Range-Corrected Density-Functional Tight-
40 Binding Method Combined with the Polarizable Continuum Model. *J. Phys. Chem. A*
41 **2019**, *123*, 5649–565.
42
43
44
45
46
47
48
49
50
51
52
53
54
55
56
57
58
59
60

- 1
2
3 (31) Heringer, D.; Niehaus, T. A.; Wanko, M.; Frauenheim, T. Analytical Excited State
4 Forces for the Time-Dependent Density-Functional Tight-Binding Method. *J. Comput.*
5 *Chem.* **2007**, *28*, 2589–2601.
6
7
8
9
10 (32) Fan, G.; Zhu, S.; Xu, H. Density-Functional Theory Study of the Interaction Mechanism
11 and Optical Properties of Flavonols on the Boron Nitride Nanotubes. *Int. J. Quantum*
12 *Chem.* **2018**, *118*, e25514.
13
14
15
16 (33) Rapacioli, M.; Simon, A.; Marshall, C. C. M.; Cuny, J.; Kokkin, D.; Spiegelman, F.;
17 Joblin, C. Cationic Methylene–Pyrene Isomers and Isomerization Pathways: Finite
18 Temperature Theoretical Studies. *J. Phys. Chem. A* **2015**, *119*, 12845–12854.
19
20
21
22 (34) Nishimoto, Y. DFTB/PCM Applied to Ground and Excited State Potential Energy
23 Surfaces. *J. Phys. Chem. A* **2016**, *120*, 771–784, PMID: 26761635.
24
25
26
27 (35) Domínguez, A.; Aradi, B.; Frauenheim, T.; Lutsker, V.; Niehaus, T. A. Extensions
28 of the Time-Dependent Density Functional Based Tight-Binding Approach. *J. Chem.*
29 *Theory Comput.* **2013**, *9*, 4901–4914.
30
31
32
33 (36) Nishimoto, Y. Time-Dependent Density-Functional Tight-Binding Method with the
34 Third-Order Expansion of Electron Density. *J. Chem. Phys.* **2015**, *143*, 094108.
35
36
37
38 (37) Kranz, J. J.; Elstner, M.; Aradi, B.; Frauenheim, T.; Lutsker, V.; Garcia, A. D.;
39 Niehaus, T. A. Time-Dependent Extension of the Long-Range Corrected Density Func-
40 tional Based Tight-Binding Method. *J. Chem. Theory Comput.* **2017**, *13*, 1737–1747.
41
42
43
44 (38) Wanko, M.; Garavelli, M.; Bernardi, F.; Niehaus, T. A.; Frauenheim, T.; Elstner, M.
45 A Global Investigation of Excited State Surfaces Within Time-Dependent Density-
46 Functional Response Theory. *J. Chem. Phys.* **2004**, *120*, 1674–1692.
47
48
49
50 (39) Job, V.; Sethuraman, V.; Innes, K. The 3500 Å $^1A_2 - X^1A_1$ Transition of Formaldehyde-
51
52
53
54
55
56
57
58
59
60

- 1
2
3 h₂, d₂, and hd: Vibrational and Rotational Analyses. *J. Mol. Spectrosc.* **1969**, *30*,
4 365–426.
5
6
7
8 (40) Clouthier, D. J.; Ramsay, D. A. The Spectroscopy of Formaldehyde and Thioformalde-
9 hyde. *Annu. Rev. Phys. Chem.* **1983**, *34*, 31–58.
10
11
12 (41) Bremond, E.; Savarese, M.; Adamo, C.; Jacquemin, D. Accuracy of TD-DFT Geometries:
13 a Fresh Look. *J. Chem. Theory Comput.* **2018**, *14*, 3715–3727.
14
15
16 (42) Christiansen, O.; Koch, H.; Jørgensen, P. Perturbative Triple Excitation Corrections to
17 Coupled Cluster Singles and Doubles Excitation Energies. *J. Chem. Phys.* **1996**, *105*,
18 1451–1459.
19
20
21 (43) Christiansen, O.; Koch, H.; Jørgensen, P. The Second-Order Approximate Coupled
22 Cluster Singles and Doubles Model CC2. *Chem. Phys. Lett.* **1995**, *243*, 409–418.
23
24
25 (44) Christiansen, O.; Koch, H.; Jørgensen, P. Response Functions in the CC3 Iterative
26 Triple Excitation Model. *J. Chem. Phys.* **1995**, *103*, 7429–7441.
27
28
29 (45) Andersson, K.; Malmqvist, P. A.; Roos, B. O.; Sadlej, A. J.; Wolinski, K. Second-Order
30 Perturbation Theory With a CASSCF Reference Function. *J. Phys. Chem.* **1990**, *94*,
31 5483–5488.
32
33
34 (46) Andersson, K.; Malmqvist, P.-A.; Roos, B. O. Second-Order Perturbation Theory With
35 a Complete Active Space Self-Consistent Field Reference Function. *J. Chem. Phys.*
36 **1992**, *96*, 1218–1226.
37
38
39 (47) Budzák, Š.; Scalmani, G.; Jacquemin, D. Accurate Excited-State Geometries: a CASPT2
40 and Coupled-Cluster Reference Database for Small Molecules. *J. Chem. Theory Comput.*
41 **2017**, *13*, 6237–6252.
42
43
44 (48) Jacquemin, D. What is the Key for Accurate Absorption and Emission Calculations ?
45 Energy or Geometry ? *J. Chem. Theory Comput.* **2018**, *14*, 1534–1543.
46
47
48
49
50
51
52
53
54
55
56
57
58
59
60

- 1
2
3 (49) Aradi, B.; Hourahine, B.; Frauenheim, T. DFTB+, a Sparse Matrix-Based Implementa-
4 tion of the DFTB Method. *J. Phys. Chem. A* **2007**, *111*, 5678–5684.
5
6
7
8 (50) Petraglia, R.; Corminboeuf, C. A Caveat on SCC-DFTB and Noncovalent Interactions
9 Involving Sulfur Atoms. *J. Chem. Theory Comput.* **2013**, *9*, 3020–3025.
10
11
12 (51) Yang,; Yu, H.; York, D.; Cui, Q.; Elstner, M. Extension of the Self-Consistent-Charge
13 Density-Functional Tight-Binding Method: Third-Order Expansion of the Density
14 Functional Theory Total Energy and Introduction of a Modified Effective Coulomb
15 Interaction. *J. Phys. Chem. A* **2007**, *111*, 10861–10873.
16
17
18
19
20
21 (52) Perdew, J. P.; Burke, K.; Ernzerhof, M. Generalized Gradient Approximation Made
22 Simple. *Phys. Rev. Lett.* **1996**, *77*, 3865–3868.
23
24
25
26 (53) Becke, A. D. Density-Functional Thermochemistry. 3. The Role of Exact Exchange. *J.*
27 *Chem. Phys.* **1993**, *98*, 5648–5652.
28
29
30
31 (54) Stephens, P. J.; Devlin, F. J.; Chabalowski, C. F.; Frisch, M. J. Ab Initio Calculation of
32 Vibrational Absorption and Circular Dichroism Spectra Using Density Functional Force
33 Fields. *J. Phys. Chem.* **1994**, *98*, 11623–11627.
34
35
36
37 (55) Barone, V.; Orlandini, L.; Adamo, C. Proton Transfer in Model Hydrogen-Bonded
38 Systems by a Density Functional Approach. *Chem. Phys. Lett.* **1994**, *231*, 295–300.
39
40
41
42 (56) Stephens, P. J.; Devlin, F. J.; Frisch, M. J.; Chabalowski, C. F. Ab initio Calculation of
43 Vibrational Absorption and Circular Dichroism Spectra Using Density Functional Force
44 Fields. *J. Phys. Chem.* **1994**, *98*, 11623–11627.
45
46
47
48 (57) Hättig, C.; Weigend, F. CC2 Excitation Energy Calculations on Large Molecules Using
49 the Resolution of the Identity Approximation. *J. Chem. Phys.* **2000**, *113*, 5154–5161.
50
51
52
53 (58) Hättig, C.; Hald, K. Implementation of RI-CC2 Triplet Excitation Energies With an
54 Application to *Trans*-Azobenzene. *Phys. Chem. Chem. Phys.* **2002**, *4*, 2111–2118.
55
56
57
58
59
60

- (59) Frisch, M. J.; Trucks, G. W.; Schlegel, H. B.; Scuseria, G. E.; Robb, M. A.; Cheeseman, J. R.; Scalmani, G.; Barone, V.; Petersson, G. A.; Nakatsuji, H.; Li, X.; Caricato, M.; Marenich, A. V.; Bloino, J.; Janesko, B. G.; Gomperts, R.; Mennucci, B.; Hratchian, H. P.; Ortiz, J. V.; Izmaylov, A. F.; Sonnenberg, J. L.; Williams-Young, D.; Ding, F.; Lipparini, F.; Egidi, F.; Goings, J.; Peng, B.; Petrone, A.; Henderson, T.; Ranasinghe, D.; Zakrzewski, V. G.; Gao, J.; Rega, N.; Zheng, G.; Liang, W.; Hada, M.; Ehara, M.; Toyota, K.; Fukuda, R.; Hasegawa, J.; Ishida, M.; Nakajima, T.; Honda, Y.; Kitao, O.; Nakai, H.; Vreven, T.; Throssell, K.; Montgomery, J. A., Jr.; Peralta, J. E.; Ogliaro, F.; Bearpark, M. J.; Heyd, J. J.; Brothers, E. N.; Kudin, K. N.; Staroverov, V. N.; Keith, T. A.; Kobayashi, R.; Normand, J.; Raghavachari, K.; Rendell, A. P.; Burant, J. C.; Iyengar, S. S.; Tomasi, J.; Cossi, M.; Millam, J. M.; Klene, M.; Adamo, C.; Cammi, R.; Ochterski, J. W.; Martin, R. L.; Morokuma, K.; Farkas, O.; Foresman, J. B.; Fox, D. J. Gaussian 16 Revision A.03. 2016; Gaussian Inc. Wallingford CT.
- (60) TURBOMOLE V6.6 2014, a development of University of Karlsruhe and Forschungszentrum Karlsruhe GmbH, 1989-2007, TURBOMOLE GmbH, since 2007; available from <http://www.turbomole.com> (accessed 13 June 2016).
- (61) Moule, D. C.; Foo, P. D. Analysis of the 2973 Å Absorption System of Phosgene. *J. Chem. Phys.* **1971**, *55*, 1262–1268.
- (62) Judge, R.; Moule, D. The $\tilde{A}^1A'' \leftarrow \tilde{X}^1A'$ Electronic Transition in Formyl Chloride, CHClO. *J. Mol. Spectrosc.* **1985**, *113*, 302–309.
- (63) Ding, H.; J. Orr-Ewing, A.; N. Dixon, R. Rotational Structure in the $\tilde{A}^1A'' - \tilde{X}^1A'$ Spectrum of Formyl Chloride. *Phys. Chem. Chem. Phys.* **1999**, *1*, 4181–4185.
- (64) Ernsting, N. P.; Pfab, J.; Romelt, J. Geometry Changes Accompanying Electronic Excitation of Nitrosomethane in the 650 nm Region. *J. Chem. Soc., Faraday Trans. 2* **1978**, *74*, 2286–2294.

- 1
2
3
4 (65) Gordon, R. D.; Luck, P. Conformational Changes Accompanying Electronic Excitation
5 of CD₃NO. *Chem. Phys. Lett.* **1979**, *65*, 480–483.
6
7
- 8 (66) Judge, R.; Moule, D. Thiocarbonyl Spectroscopy: The $\tilde{A}^1A'' \leftarrow \tilde{X}^1A'$ and $\tilde{a}^3A'' \leftarrow \tilde{X}^1A'$
9 Electronic Transitions in Thioformyl Chloride, CHClS. *J. Mol. Struct.* **1985**, *113*, 77–84.
10
11
- 12 (67) Bokarev, S. I.; Dolgov, E. K.; Bataev, V. A.; Godunov, I. A. Molecular Parameters of
13 Tetraatomic Carbonyls X₂CO and XYCO (X, Y = H, F, Cl) in the Ground and Lowest
14 Excited Electronic States, Part 1: A Test of Ab Initio Methods. *Int. J. Quantum Chem.*
15 **2009**, *109*, 569–585.
16
17
- 18 (68) Jensen, P.; Bunker, P. The Geometry and the Inversion Potential Function of Formalde-
19 hyde in the \tilde{A}^1A_2 and \tilde{a}^3A_2 Electronic States. *J. Mol. Spectrosc.* **1982**, *94*, 114–125.
20
21
- 22 (69) Dallos, M.; Müller, T.; Lischka, H.; Shepard, R. Geometry Optimization of Excited Va-
23 lence States of Formaldehyde Using Analytical Multireference Configuration Interaction
24 Singles and Doubles and Multireference Averaged Quadratic Coupled-Cluster Gradients,
25 and the Conical Intersection Formed by the $1^1B_1(\sigma - \pi^*)$ and $2^1A_1(\pi - \pi^*)$ States. *J.*
26 *Chem. Phys.* **2001**, *114*, 746–757.
27
28
- 29 (70) Hubbard, L. M.; Bocian, D. F.; Birge, R. R. The Nature of the $^1n\pi^* \leftarrow S_0$ Transition.
30 4. The First Excited Singlet State of Acetaldehyde. *J. Am. Chem. Soc.* **1981**, *103*,
31 3313–3320.
32
33
- 34 (71) Guido, C. A.; Jacquemin, D.; Adamo, C.; Mennucci, B. On the TD-DFT Accuracy in
35 Determining Single and Double Bonds in Excited-State Structures of Organic Molecules.
36 *J. Phys. Chem. A* **2010**, *114*, 13402–13410.
37
38
- 39 (72) Bousquet, D.; Fukuda, R.; Maitarad, P.; Jacquemin, D.; Ciofini, I.; Adamo, C.; Ehara, M.
40 Excited-State Geometries of Heteroaromatic Compounds: A Comparative TD-DFT and
41 SAC-CI Study. *J. Chem. Theory Comput.* **2013**, *9*, 2368–2379.
42
43
44
45
46
47
48
49
50
51
52
53
54
55
56
57
58
59
60

- 1
2
3
4 (73) Guareschi, R.; Filippi, C. Ground- and Excited-State Geometry Optimization of Small
5 Organic Molecules with Quantum Monte Carlo. *J. Chem. Theory Comput.* **2013**, *9*,
6 5513–5525.
7
8
9
10 (74) Brémond, É.; Savarese, M.; Su, N. Q.; Pérez-Jiménez, Á. J.; Xu, X.; Sancho-García, J. C.;
11 Adamo, C. Benchmarking Density Functionals on Structural Parameters of Small-
12 /Medium-Sized Organic Molecules. *J. Chem. Theory Comput.* **2016**, *12*, 459–465.
13
14
15
16 (75) Tuna, D.; Lu, Y.; Koslowski, A.; Thiel, W. Semiempirical Quantum-Chemical
17 Orthogonalization-Corrected Methods: Benchmarks of Electronically Excited States. *J.*
18 *Chem. Theory Comput.* **2016**, *12*, 4400–4422.
19
20
21
22
23 (76) Köhn, A.; Hättig, C. Analytic Gradients for Excited States in the Coupled-Cluster
24 Model CC2 Employing the Resolution-Of-The-Identity Approximation. *J. Chem. Phys.*
25 **2003**, *119*, 5021–5036.
26
27
28
29 (77) Hättig, C. In *Response Theory and Molecular Properties (A Tribute to Jan Linderberg*
30 *and Poul Jørgensen)*; Jensen, H. A., Ed.; Advances in Quantum Chemistry; Academic
31 Press, 2005; Vol. 50; pp 37–60.
32
33
34
35
36 (78) Suellen, C.; Garcia Freitas, R.; Loos, P.-F.; Jacquemin, D. Cross Comparisons Between
37 Experiment, TD-DFT, CC, and ADC for Transition Energies. *J. Chem. Theory Comput.*
38 **2019**, doi: 10.1021/acs.jctc.9b00446.
39
40
41
42
43
44
45
46
47
48
49
50
51
52
53
54
55
56
57
58
59
60

Graphical TOC Entry

